PNAS RESEARCH ARTICLE | ECOLOGY

Changes in the functional diversity of modern bird species over the last million years

Ryan R. Germain[a,b,1], Shaohong Feng[c,d,e], Lucas Buffan[f], Carlos P. Carmona[g], Guangji Chen[c,h], Gary R. Graves[a,i], Joseph A. Tobias[j], Carsten Rahbek[a,k,l,m], Fumin Lei[n], Jon Fjeldså[a,o], Peter A. Hosner[a,k,o], M. Thomas P. Gilbert[p,q], Guojie Zhang[b,c,d,e,r,1], and David Nogués-Bravo[a,1]

Edited by Jenny L. McGuire, Georgia Institute of Technology, Atlanta, Georgia; received March 7, 2022; accepted October 28, 2022 by Editorial Board Member Nils C. Stenseth

Despite evidence of declining biosphere integrity, we currently lack understanding of how the functional diversity associated with changes in abundance among ecological communities has varied over time and before widespread human disturbances. We combine morphological, ecological, and life-history trait data for >260 extant bird species with genomic-based estimates of changing effective population size (N_e) to quantify demographic-based shifts in avian functional diversity over the past million years and under pre-anthropogenic climate warming. We show that functional diversity was relatively stable over this period, but underwent significant changes in some key areas of trait space due to changing species abundances. Our results suggest that patterns of population decline over the Pleistocene have been concentrated in particular regions of trait space associated with extreme reproductive strategies and low dispersal ability, consistent with an overall erosion of functional diversity. Further, species most sensitive to climate warming occupied a relatively narrow region of functional space, indicating that the largest potential population increases and decreases under climate change will occur among species with relatively similar trait sets. Overall, our results identify fluctuations in functional space of extant species over evolutionary timescales and represent the demographic-based vulnerability of different regions of functional space among these taxa. The integration of paleodemographic dynamics with functional trait data enhances our ability to quantify losses of biosphere integrity before anthropogenic disturbances and attribute contemporary biodiversity loss to different drivers over time.

functional traits | functional diversity | trait space | paleodemography | effective population size

Significance

Combining genomic-based estimates of past effective population sizes for >260 extant species and comprehensive datasets of species-specific traits, we reconstruct patterns of avian functional diversity over the last million years and under pre-anthropogenic climate warming. Our results suggest an overall preservation of functional diversity over this time, but with a significant erosion of functional diversity across peripheral regions of functional space representing more extreme trait sets. Species most sensitive to climate warming occupied more redundant areas of trait space, but overall functional diversity declined significantly during this relatively short period of the Pleistocene. Our approach provides a major step forward in understanding temporal dynamics in functional diversity before humans began to exert broad-scale effects on the biosphere.

The safeguarding of biological diversity is one of the society's most pressing challenges (1), but our understanding of its decline and consequences is still limited and often constrained by the spatial and temporal scales at which natural history studies are conducted. Despite such constraints, novel opportunities exist for using information from the Quaternary period (~2.6 Mya–present) to inform conservation practices and policies in the context of climate change, including providing natural baselines of biotic responses and quantifying the vulnerability of the natural world to varying rates and magnitudes of climate change (2). Exploring biodiversity responses during pre-human periods allows us to more clearly infer the impact of climate change without the additional effects of other anthropogenic pressures and thus tackle some of the challenges posed by the difficulty in accurately attributing observed changes to different drivers of biodiversity change (3–5). This "attribution conundrum" exists in part because collinearity, scale dependencies, or interactions among the different potential drivers of biodiversity change (e.g., ongoing climate change, habitat loss, over-exploitation) may obscure their individual effects on species declines across taxa.

In addition to their overall effects on species declines across taxa, drivers of biodiversity change can also cause changes in the relative abundance of different species, shifting representation of key functional traits (i.e., the morphological, behavioral, or physiological features of organisms that can affect their fitness) in communities and leading to overall erosion of functional diversity (i.e., the variation among such features) over time (6–8). The loss of functional diversity associated with both species extinctions and overall declines in abundance can lead to declines in the functioning and stability of ecosystems over time, particularly during periods of broad-scale environmental variation such as climate change (9–11). An overrepresentation of species exhibiting similar traits can buffer these effects of declining abundances, allowing key ecosystem functions to be maintained during periods of biodiversity loss. Indeed, over the past century, changes in species abundances are more prevalent than global extinctions (12–15), emphasizing the need to incorporate estimates of species abundances in analyses of global functional diversity change (16). By identifying changes in representation across avian functional space (i.e., multi-dimensional

Author contributions: R.R.G., G.Z., and D.N.-B. designed research; R.R.G. performed research; R.R.G., S.F., L.B., and C.P.C. analyzed data; G.C., G.R.G., J.A.T., C.R., F.L., J.F., P.A.H., M.T.P.G., and G.Z. assembly of genomic and trait data; and R.R.G., S.F., L.B., C.P.C., G.C., G.R.G., J.A.T., C.R., F.L., J.F., P.A.H., M.T.P.G., G.Z., and D.N.-B. wrote the paper.

The authors declare no competing interest.

This article is a PNAS Direct Submission. J.L.M. is a guest editor invited by the Editorial Board.

[1]To whom correspondence may be addressed. Email: ryan.germain@bio.ku.dk, guojie.zhang@bio.ku.dk, or dnogues@sund.ku.dk.

This article contains supporting information online at https://www.pnas.org/lookup/suppl/doi:10.1073/pnas.2201945119/-/DCSupplemental.

Published February 6, 2023.

space where species are grouped based on their functional traits) during the Pleistocene epoch (~2.6 Mya – 11.7 thousand years ago [kya]), we aim to provide baseline estimates of functional diversity within avian communities before the widespread effects of humans on global wildlife. Doing so will identify the regions of functional space that are more resilient or more sensitive to climate warming, thus helping provide more plausible scenarios for future changes in avian functional diversity.

Current understanding of global and regional dynamics in functional diversity is limited due to missing information about the past abundances of species (2, 17). This missing information hampers our ability to estimate baselines before human impacts and to quantify the magnitude and rates of ongoing losses of functional diversity and associated ecosystem functioning during periods of rapid environmental change. The modern genomic revolution offers a unique opportunity to investigate how demographic changes may have affected functional diversity over the Earth's history. In particular, species-specific estimates of changing effective population size (N_e) over thousands-to-millions of years, inferred from whole-genome sequence data (18), can provide key estimates of fluctuations in abundance over evolutionary time and across biogeographic realms. Coupling such information with morphological, life-history, and ecological trait data for a broad selection of species permits reconstruction of the representation (in terms of abundance) of different functional traits over different periods of the distant past, revealing trait sets associated with functional diversity across a dynamically changing global environment. For instance, the last million years on Earth have been punctuated by periods of intense climate warming and cooling (19, 20). A recent analysis of genomic data in birds revealed that while overall bird abundance has steadily declined over the past million years, certain sets of morphological/life-history traits were associated with either species-specific population increases or decreases during discrete periods of climate warming and cooling (21). These observations suggest that the functional diversity of avian communities also fluctuates over time and during periods of climate variation. Identifying regions of functional space that are less occupied in more recent time periods due to population declines of certain species can provide baseline information on the diversity and composition of long-term ecological strategies leading up to the modern Holocene epoch (~11 kya–present). Such information will also illuminate regions of the global functional trait space which may be less resilient to future environmental challenges, beyond those documented under contemporary studies of population responses to current climate change.

Here, we combine morphological, ecological, and life-history trait data for >260 extant bird species with estimates of changing N_e to quantify shifts in avian functional diversity over the past million years and explore patterns of change over time and space. We reconstruct the abundance-weighted functional trait space of these bird species in three time periods to quantify how functional diversity has changed 1) over time, 2) across the Earth's major zoogeographic realms, and 3) how abundances have shifted across the avian functional space to potentially influence these patterns. We further quantify changes in functional diversity during the most recent period of abrupt climate warming over the past million years to identify the areas of the functional space most sensitive to broad-scale climate warming.

Results

Changes in Occupation of Functional Trait Space Over Time. Principal component analysis (PCA) of six key morphological/life-history traits associated with long-term demographic change identified two principal components (PCs) that explain 77.6% (PC1 = 56.95%, PC1 = 20.60%) of the variance in avian functional trait space among 263 species (Fig. 1*A*). Within this functional space, the main axis of variation ran from smaller-bodied species with smaller eggs and shorter incubation times to larger species with larger eggs and longer incubation times (left to right in each panel of Fig. 1*A*; more strongly associated with PC1 than PC2). The secondary axis of variation ran from species with large clutch sizes and a smaller hand-wing index (indicative of reduced dispersal ability; see *Methods*) to small-clutched species with a larger hand-wing index (*Upper* to *Lower* section in each panel of Fig. 1*A*; more strongly associated with PC2 than PC1).

Trait probability densities (TPDs), calculated via abundance-weighted PC values, varied among three equal time periods (1 Mya–666 kya, 665–333 kya, 332–30 kya) over the past million years, but revealed that small-bodied species with smaller clutches and a smaller hand-wing index were consistently more abundant and represent a "hotspot" in functional trait space (Fig. 1*A*). Estimates of functional "redundancy" (measured here as over- or underrepresentation of species compared to null expectations) within such core portions of the functional trait space remained similar across the three time periods (*SI Appendix*, Fig. S1). However, occupancy within peripheral portions of the functional space gradually eroded from more ancient time through more recent time (Fig. 1*A*), revealing an overall decrease in abundance of larger-bodied species with a smaller hand-wing index (e.g., larger PC1 and PC2 values, upper arrow in Fig. 1*A*), as well as an overall decrease in large-bodied species with longer incubation durations and a larger hand-wing index (i.e., larger PC1 and lower PC2 values, lower arrow in Fig. 1*A*). Comparisons of TPD dissimilarity indices to null expectations highlighted significant differences in TPDs between Time 3 (1 Mya–666 kya) and Time 2 (665–333 kya; Standardized Effect Size [SES] = 3.46 $P < 0.01$) and Time 2 and Time 1 (332–30 kya; SES = 4.33, $P < 0.01$), thereby confirming that functional diversity gradually shifted between each of three focal time periods. Overall dissimilarity across the entire study (Time 3 to Time 1) was strongly significant (SES = 7.66, $P < 0.001$; Fig. 1*B*) and was the result of both declines and increases across different portions of the global functional trait space (Fig. 1*C*). We detected overall declines in representation among smaller-bodied species with smaller eggs and larger clutch sizes from more ancient time to more recent time, as well as overall increases among large-bodied species with longer incubation durations and a larger hand-wing index, indicative of stronger dispersal ability (Fig. 1*C*). Despite this, there were clear pockets of changing representation along each PC axis, rather than an overall gradient of increase/decline along each axis of variation (e.g., both increases and decreases among larger-bodied species). Thus, the nuances of change in functional diversity of birds over the past million years are best captured through consideration of whole-phenotypic variation and each species' position in multi-dimensional trait space, rather than their position along individual axes of functional variation.

Changes in Occupation of Functional Trait Space across Zoogeographic Realms. Changes in functional diversity from the ancient past (Time 3) to the more recent past (Time 1) varied among the Earth's major zoogeographic realms, where occupation of different portions of the functional space shifted over time (Fig. 2*A*). Realm-specific changes revealed varying trait-based vulnerabilities to demographic change, with the erosion of multiple hotspots of functional diversity over time (*SI Appendix*, Fig. S2). Overall dissimilarity in occupation of functional space over the last million years appears highest in the Sino-Japanese

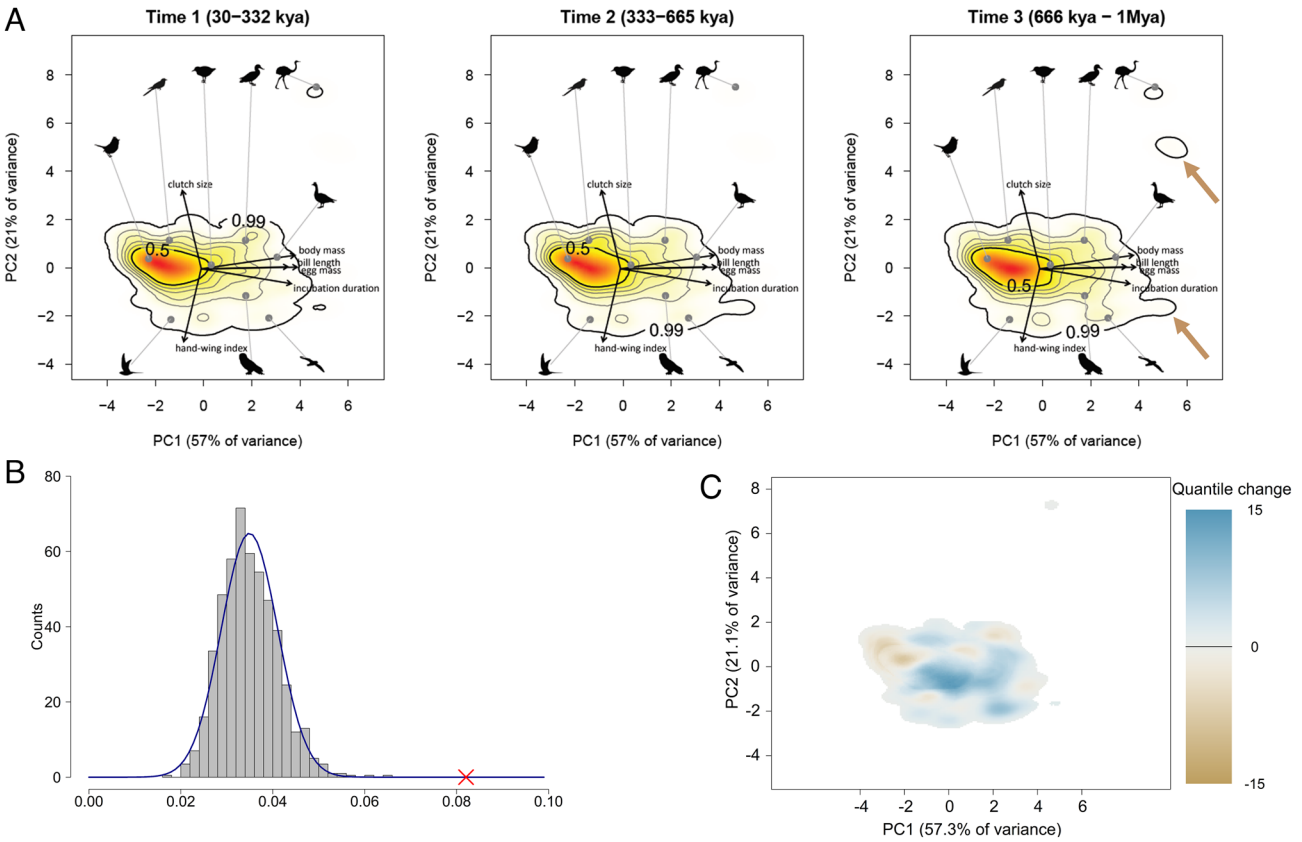

Fig. 1. Changes in occupation of the functional trait space of 263 bird species across three time periods over the last one million years. (*A*) Trait probability densities (TPDs), calculated via abundance-weighted PCA of six key morphological/life-history traits (arrows illustrate direction and weighting of each trait along PC1 and PC2), depicting probabilistic distributions of species in functional trait space. Contour lines and color gradients represent density of species in the defined space, where 50% (0.5) of all species analyzed fall with the "hotspot" depicted by the first contour (red) and subsequent lines indicate the 0.6, 0.7, 0.8, 0.9, and 0.99 quantiles. Brown arrows in *Rightmost* panel depict peripheral regions of functional space which have eroded over the past million years (see *Results*). (*B*) Distribution of overall dissimilarity indices between TPDs from Time 3 and Time 1, based on randomly generated abundances for each species in each time period (n = 1000 iterations). The observed value of dissimilarity between Time 3 and Time 1 is demarcated by the red "X" along the x-axis. (*C*) Overall changes in functional diversity over time (expressed in quantiles), measured as differences in TPDs between Time 1 and Time 3. Brown tones represent areas of the functional trait space that are more densely occupied in the distant past (Time 3) and have thus decreased over time. Blue tones represent areas that more densely occupied in the more recent past (Time 1) and have thus increased over time.

and Afrotropical realms, and lowest in the Oriental, Nearctic, and Panamanian realms (Fig. 2*B*). For the majority of realms, such changes in functional diversity were smaller more recently (Time 2 to Time 1) than in the distant past (Time 3 to Time 2), with the largest change occurring in the Sino-Japanese realm between Time 3 and Time 2 (though note the relatively small sample size within this realm; Fig. 2*B*). Despite these fluctuations in functional diversity over time, overall changes in species-specific abundances remained relatively similar across realms, with only Nearctic and Sino-Japanese species exhibiting significant increases in mean N_e between Time 3 and Time 2, whereas no significant changes occurred between Time 2 and Time 1 (*SI Appendix*, Fig. S3). Although somewhat speculative given the uneven sample sizes among realms, this relative consistency of change across realms may indicate that overall changes in functional diversity (Fig. 1 *A*–*C*) represent fluctuations in global avian community composition over time, rather than dramatic increases or decreases in population size within species groups occupying certain geographic regions.

Representation of Categorical Traits Over Time. Analysis of species-specific abundances revealed shifting representation of key traits describing different ecological and life-history strategies over time. Global models describing species-specific N_e across categorical trait groups represented relatively good fits to the data for 280 species across all three time periods (Time 1: R^2 = 0.12, Time 2: R^2 = 0.13, Time 3: R^2 = 0.10) and top-model subsets (within ΔAIC ≤ 7 from the best-fitting model) for Time 1, Time 2, and Time 3 consisted of n = 12, 14, and 15 models, respectively (*SI Appendix*, Table S1). Final averaged models revealed both shifting representation of some key traits from more ancient time to more recent time, as well as consistently higher or lower representation of other trait groups over the past one million years (Fig. 3). Specifically, abundance was linked to main diet type in the more ancient time periods, where species whose main diet consisted of either fruit, seeds, invertebrates, or plant material exhibited significantly higher mean N_e than species with other main diet types in both Time 2 and Time 3. However, main diet was not associated with N_e in the final averaged model for Time 1. Similarly, migratory species were more represented in Time 1 and Time 2, but migration strategy was not significantly associated with abundance in Time 3. Further, semi-precocial or semi-altricial species were less abundant in Time 1, but developmental mode was not associated with abundance in more ancient time periods. In contrast to these shifting associations, broad taxonomic classification was consistently linked to abundance across Time 1, Time 2, and Time 3, where waterbirds and raptors exhibited significantly lower mean N_e than other taxonomic groups over the past million years (Fig. 3).

Changes in Occupation of Functional Space during Climate Warming. TPDs, once again calculated via abundance-weighted PC values, varied significantly between the beginning and end of

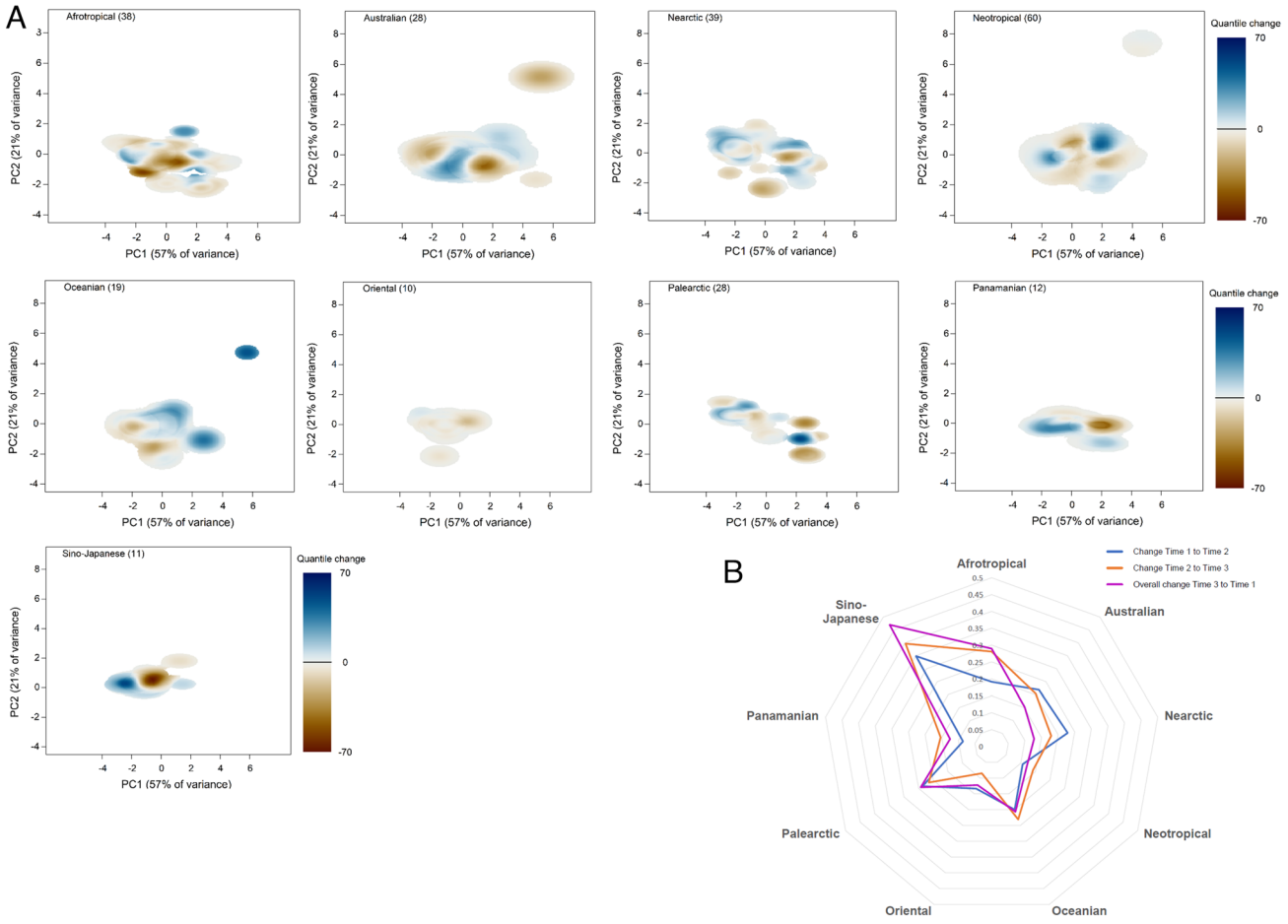

Fig. 2. Changes in avian functional diversity across the Earth's major zoogeographic realms. (*A*) Overall changes in functional diversity over time (expressed in quantiles) in each realm, measured as differences in TPDs between Time 1 and Time 3 (see SI *Appendix*, Fig. S1 for TPDs for each realm during each time period). Brown tones represent areas of the functional trait space that are more densely occupied in the distant past (Time 3) and have thus decreased over time. Blue tones represent areas that more densely occupied in the more recent past (Time 1) and have thus increased over time. A number of species included in analysis of each realm are given in parentheses. (*B*) Radar plot depicting dissimilarity indices between TPDs in each of the three time periods in each zoogeographic realm. Overall dissimilarity in functional diversity over the entire study period (Time 3 [ancient] to Time 1 [recent]) for each realm is presented in purple, whereas sequential changes in trait space between Time 3 and Time 2, and Time 2 and Time 1 are presented in orange and blue, respectively. Each contour line represents an increase in dissimilarity index of 0.5. See SI *Appendix*, Fig. S2*A* for visual representation of zoogeographic realms, as defined by Holt et al. (22).

one of the most recent periods of climate warming over the past million years (~147–123 kya), revealing that broad-scale changes in functional diversity can also occur during relatively short periods of intense environmental change. This warming event represents a change of ~8°C in Global Average Surface Temperature from modern levels (19) and thus offers key insight into the baseline direction and magnitude of functional change that can occur over the next several centuries due to climate warming alone, independent of additional anthropogenic stressors. In particular, the largest increases and declines in abundance occurred among species occupying relatively similar areas of functional space (i.e., smaller-bodied species with smaller egg masses, shorter incubation durations, larger clutches, and lower hand-wing indexes; Fig. 4*A*), compared to the more broadly distributed changes in functional space across the past million years (Fig. 1*C*). Despite such subtle changes in occupation of functional space, dissimilarity indexes between the beginning and end of this period of climate warming differed significantly from null expectations (SES = 5.29, $P < 0.01$; Fig. 4*B*)

Discussion

Building on the largest reconstruction of avian paleodemography yet available (21) and newly assembled comparative datasets of a broad range of species-specific traits (23), we show that avian functional diversity was relatively stable over the last million years. However, we also found that significant changes in representation have occurred among key regions of demographic-based functional space during this period of the mid-to-late Pleistocene, indicating that a large proportion of levels of functional redundancy were intact before the global expansion of humans. In addition to these long-term changes in functional diversity among extant bird species, we also identified the region of functional space most sensitive to changes in abundance during one of the most recent climate warming events (~147–123 kya). These findings provide relevant baselines for avian functional diversity before widespread human influence, but may also help inform scenarios to anticipate and quantify the functional diversity consequences of future climate change.

While birds exhibit a wide variety of trait sets that enable them to engage in numerous and important ecosystem functions, including seed dispersal, pollination, control of insect populations, and the consumption of dead animals (24), we found that avian functional space over the last million years was largely defined by a limited set of trait combinations and ecological or life-history strategies. Fluctuations in functional diversity over time thus appear to be triggered by changes in demographic-based representation of peripheral regions of functional space representing less common trait combinations and a limited number of categorical trait groups.

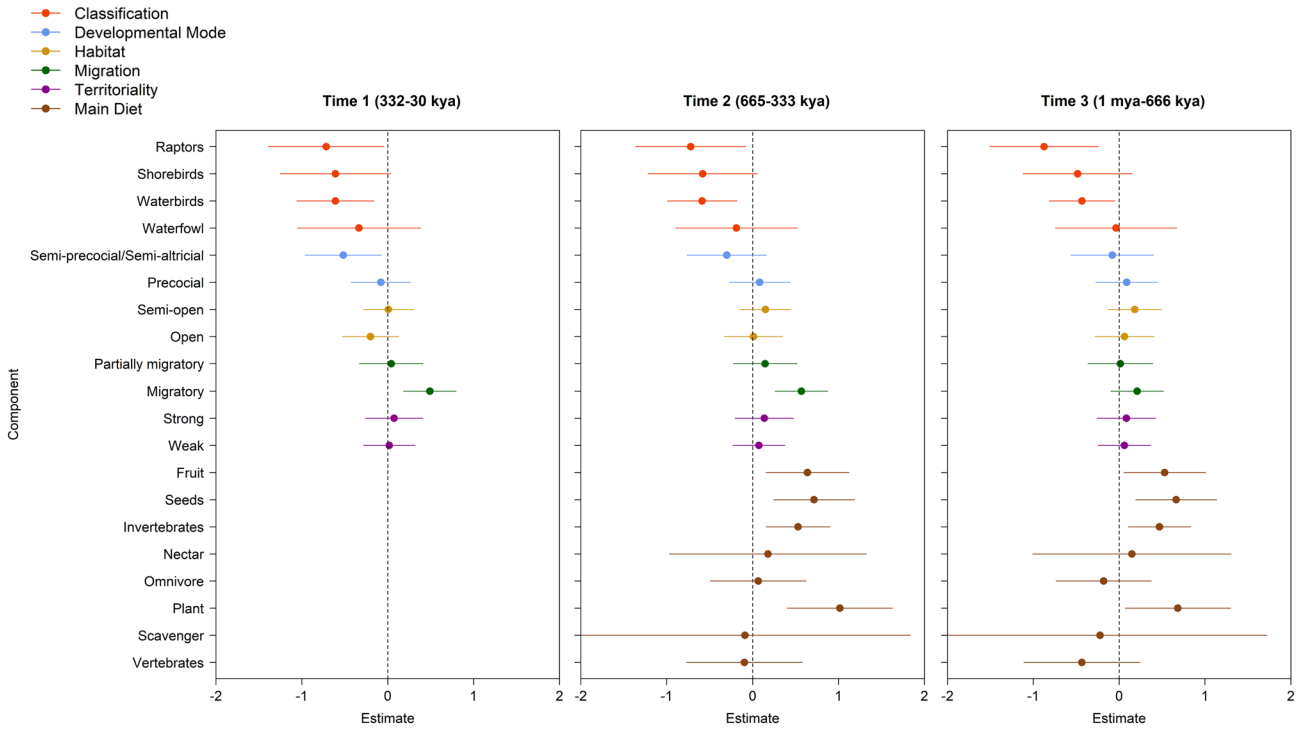

Fig. 3. Parameter estimates (± 95% confidence intervals) from final averaged models of representation (in terms of species-specific abundances) among ecological traits groups over the past one million years. Statistical significance for each group within each categorical trait was assessed by whether lower or upper confidence intervals overlapped zero. Note that "Main Diet' was not included in the Δ AIC ≤ 7 subset for Time 1 (*SI Appendix*, Table S1), and thus parameter estimates for groups within this categorical trait are blank. Estimates are color-coded by categorical trait (legend). Sample sizes for each group level within each trait are provided in *SI Appendix*, Table S2. Note that the model intercept represents the first group level in each categorical trait (i.e., classification = landbirds, developmental mode = altricial, habitat type = dense, migratory strategy = sedentary, territoriality = none, main diet = aquatic invertebrates), and thus estimates from these groups are not depicted.

Remarkably different morphological forms and life-history strategies often co-occur within ecosystems, but no single form or strategy can optimize reproductive output and abundance over time (25). Our observed changes in abundance of highly differentiated bird strategies over the past million years (Fig. 1*C*) support such theory regarding the coexistence of multiple and even contrasting strategies optimizing demographic representation. The relative position of species in functional space strongly determined how their abundance changed between the most ancient and most recent time periods; however, detecting such changes required considering multiple dimensions of functional variation simultaneously, as species with similar values for one dimension of variation (e.g., body size) exhibited highly contrasting responses depending on additional morphological traits and/or life-history strategies. For instance, regions of functional space representing species with larger body sizes and a larger hand-wing index (indicative of stronger dispersal ability; e.g., Northern fulmar—*Fulmarus glacialis*; Cory's shearwater—*Calonectris borealis*; Golden eagle—*Aquila chrysaetos*) increased in relative abundance from more ancient (Time 3) to more recent (Time 1) periods (Fig. 1*C*). In contrast, we detected

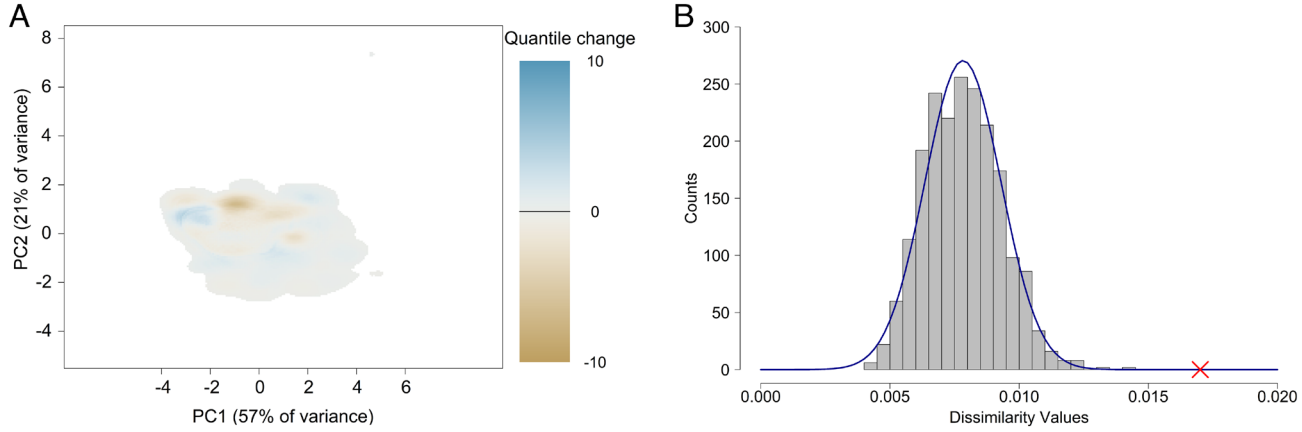

Fig. 4. Changes in occupation of the functional trait space of 263 bird species from the beginning to the end of the period of climate warming from ~147–123 kya. (*A*) Overall changes in functional diversity over time (expressed in quantiles), measured as differences in TPDs between the "warming start" and "warming end" periods. Brown tones represent areas of the functional trait space that are more densely occupied at the start of the warming period and have thus decreased with climate warming. Blue tones represent areas that more densely occupied at the end of the warming period and have thus increased with climate warming. (*B*) Distribution of overall dissimilarity indices between "warming start" and "warming end," based on randomly generated abundances for each species in each time period (n = 1000 iterations). The observed value of dissimilarity (0.017) is demarcated by the red "X" along the x-axis.

decreases in relative abundance over time in large-bodied species with larger clutches and a relatively lower hand-wing index (e.g., Emu—*Dromaius novaehollandiae*; Southern cassowary—*Casuarius casuarius*; Swan Goose—*Anser cygnoid*). In addition to this variation associated with dispersal ability, we found that migratory species were better represented in terms of overall abundance than partially migratory or resident species during more recent time periods (Fig. 3). Recent work indicates that long-distance migrants are able to shift their distribution to better match climate refugia during glacial periods, resulting in little negative effects on population size over glacial/interglacial cycles (26). Our findings concur that migratory species and those exhibiting proxies for stronger dispersal ability exhibited long-term increases in abundance compared to more sedentary species over the Pleistocene, a period punctuated by dramatic climate variation (19, 20). We further determined that semi-precocial/semi-altricial species declined over time (i.e., significantly underrepresented in Time 1; Fig. 3), despite the fact that species with longer incubation durations tended to increase from more ancient to more recent time (Fig. 1*C*). These and other results across various taxonomic plant and animal groups (7, 27, 28) highlight the importance of considering multiple axes of continuous and categorical functional variation, and thus similar or co-occurring life-history strategies, when examining past or projecting future changes in abundance across communities.

A key aspect of safeguarding biological diversity requires maintaining high levels of species which contribute similar roles to ecosystem functioning (i.e., functional redundancy) to avoid critical losses of functions following the declines and extinctions of individual species. Since the mid-1990s, ecologists have been exploring the effects of species loss on overall ecosystem functioning, ecosystem stability, nutrient balance, and productivity (29–33). However, in terms of practical conservation outcomes, functional redundancy has been considered a "double-edge sword" (34) because functionally redundant species may be considered more expendable, in that their loss will have minimal impact on ecosystem functions. Research over the last decade has demonstrated that the representation of species occupying similar regions of functional space, and thus contributing similar roles to ecosystem functioning, is a critical aspect of the resilience of biological diversity to global change (7, 35, 36). Therefore, functional diversity has become a major focus in conservation tools and policies. The Essential Biodiversity Variables (37) for example include community composition and ecosystem functioning as key measurements to study and manage biodiversity, and functional diversity is also an integral part of the IUCN Red List of Ecosystems (38). We found that functional redundancy has remained broadly stable over the Pleistocene (*SI Appendix*, Fig. S1), with the largest representation of species in functional trait space (i.e., "hotspots") occurring among smaller birds with shorter incubation times and slightly larger clutch sizes (Fig. 1*A* and *SI Appendix*, Fig. S1). This represents a nearly universal pattern among taxonomic groups, where smaller, more fecund species tend to be better represented in functional trait space (6, 7, 36, 39). Thus, while the largest overall declines in abundance have occurred among such species (Fig. 1*C*), their overrepresentation may buffer ecosystem functioning to long-term declines in global bird abundance both over the past million years (21) and more recently (15). We further observed that peripheral regions of functional space (e.g., those representing larger-bodied, less-fecund species with stronger dispersal ability) gradually eroded over time (Fig. 1 *A* and *C*). These findings suggest that while a large proportion of levels of functional redundancy (and the stability of ecosystem functioning that it provided) was intact before the end of the Pleistocene, there has likely been an overall decline of ecosystem functioning related to the declining abundance of some large species, even before the significant onset of human-related disturbance during the modern Holocene epoch. This overall downsizing, in terms of body size, of ecological communities across thousands of years is a recurrent pattern among vertebrates (7), particularly in mammals, and has triggered multiple instances of changing community composition and ecosystem functioning in the past (40, 41).

In addition to these long-term changes in functional diversity among bird species, we also identified the region of the functional space representing species which have undergone the strongest declines and increases in abundance during one of the most intense periods of pre-anthropogenic climate warming (~147–123 kya). Unlike observed changes in functional diversity over the past million years (Fig. 1*C*), the largest increases and decreases in occupation of functional space during this period of climate warming occurred among species with relatively similar trait sets (Fig. 4*A*). Thus, the significant changes in overall functional diversity (Fig. 4*B*) observed during this period cannot be easily assigned to one or several axes of trait variation. Instead, long-term population responses to climate warming are likely determined by a complex series of trait interactions that dictate how relatively similar species may react differently to periods of abrupt climate change (21). Such results further highlight the importance of incorporating long-term demographic changes (i.e., over evolutionary timescales) when testing hypotheses regarding how species will respond to broad-scale global environmental change.

Estimating spatial and temporal changes in abundance-weighted functional diversity provides an empirical context for exploring numerous questions related to life-history theory under global change. Here, our two dimensions of avian functional trait space broadly reflect the *r* versus *K* (i.e., "fast" versus "slow" life-histories) selection continuum (42) and how different dimensions of species representation across this continuum have shifted over the last million years. By placing different groupings of bird species (e.g., by habitat type, diet, migration strategy, developmental mode, or current conservation status) within this functional space, we can observe temporal dynamics of functional diversity in light of demographic changes in different regions of the world. The recent and ongoing erosion of functional diversity has been explored across a variety of taxa, particularly in response to modern anthropogenic drivers of biodiversity loss (6, 7, 10). For instance, over only the last 50 y, declines in bird abundance across North America have not only affected rare or threatened species, but rather represent widespread population declines across phylogenetic families and ecosystems (15). Estimates of past extinction rates and projections of future functional diversity for birds at a global scale also show that larger-bodied species with later fledging ages, longer incubation times, and lower dispersal ability (i.e., *K*-selected "slow" life-histories) are more susceptible to extinction than smaller species with faster breeding times, suggesting that the variety of life-history strategies among these threatened groups are particularly vulnerable to be lost (7, 43). However, to date, knowledge of if and how such shifts in avian functional diversity have occurred in the distant past has remained limited. Our findings that such vulnerable species represent rarer regions of avian functional space that have gradually eroded over the past million years highlight the need for increased conservation efforts to safeguard their potentially critical contributions to ecosystem functioning.

Estimating past abundances of species for analysis of global functional diversity opens exciting venues for future research, but remains challenging. To date, estimates of past demographic change based on fossil remains have been exceedingly difficult to obtain, in part due to limited fossilization potential across many species and ecosystems, particularly within the tropics (44, 45). The genomic revolution and subsequent development of coalescence theory and methods have contributed to partly overcome such limitations, allowing for robust

estimates of long-term demographic change from whole-genome sequence data (18). However, while genomic sampling for our study stems from one of the largest cross-species efforts among any vertebrate or plant group (46), and the selection of species included in our analyses covers a wide spectrum of avian taxonomic, morphological, and geographic diversity, there remain thousands of species that are yet to be sequenced. To match the extensive collection and dissemination of functional and morphological trait data now released for all extant bird species (23), an acceleration of genomic sequencing in birds, both in terms of methodology and number of species, is of utmost importance. For instance, the temporal resolution that many current methods can achieve for estimates of demographic change is so far unable to detect centennial-to-decadal changes in abundance and related functional diversity, thus reducing the potential to establish parallels and conservation lessons for the current abrupt changes in species abundances we are witnessing around the globe (2, 20). While newly developed methods may offer a path to overcoming these obstacles and estimating N_e changes within the past ~100 generations, they require increased genomic sampling from more individuals within/among populations (47), which may not always be feasible for rarer species. Working toward this target of paired high-resolution genomic and functional trait data for all bird species will usher in a new generation of broad-scale comparative analyses with implications for conservation action by exploring the impacts of rapid environmental change on avian resilience over longer timescales and up to the present era (48).

The functioning of ecosystems, their resilience to change, and the services they provide are related to the functional diversity of their constituent species (49). Our temporally explicit approach, using over 260 bird species and representing all major avian orders and a global distribution, provides baseline information of functional diversity leading into the modern period of human-induced biodiversity change referred to as the Anthropocene. These findings help to reveal the magnitude and direction of changes in functional diversity and uncover the most sensitive regions of the avian functional space to climate warming. Over a large part of the Pleistocene, the overall functional diversity of bird species has remained largely stable, but with significant changes in some of the rarest areas of functional trait space. This suggests the overall preservation of similar levels of functional diversity over the past million years likely reduces the potential for declines in ecosystem resilience. However, specific regions of functional space have shown substantial declines in demographic-based representation, even before humans began to exert broad-scale effects on the biosphere. Based on our retrospective approach among extant species, smaller-bodied species with larger clutches, smaller eggs, shorter incubation durations, and lower dispersal ability are expected to be prone to the largest changes in abundance under future warming. In light of such findings, the integration of paleodemographic dynamics with functional trait data will enhance our understanding of functional diversity and help improve estimates of biodiversity declines over time.

Materials and Methods

Genomic-Based Estimates of Demographic Change Over One Million Years. Species-specific estimates of N_e over the past million years were estimated using the Pairwise Sequential Markovian Coalescent (PSMC) method (18) applied to whole-genome sequence data, following Germain et al. (21). We used whole-genome sequencing data for 345 extant bird species assembled by Feng et al. (46) as part of the Bird 10,000 Genomes (B10K) Project (https://b1ok.genomics.cn). This represents a dense taxonomic sampling scheme of >90% of bird families, with the intention of representing a large portion of avian genomic and functional trait diversity. As part of this previous study, genomes for each species were consistently sequenced and assembled to minimize potential error due to bioinformatics artifacts, and heterozygous information for each species was inferred based on a BWA+GATK pipeline (18, 50). We applied four filtering steps to obtain high-quality SNPs, including a) removing homozygous SNPs and SNPs with more than two alternative alleles, b) removing SNPs with an interval below 10bp, c) removing SNPs with a read depth below 1/3 or over twice the average read depth across the genome, and d) removing SNPs with a root mean square mapping quality lower than 25 (51). We used branch-specific estimates of the substation rate per site (R) as proxies for mutation rate (μ) and estimated divergence times (t) via MCMCTree applied to fossil records (52–54), both provided from the most up-to-date avian phylogeny using B10k resources. We then scaled specifics-specific mutation rates to mutation rate per site per generation as $\mu = \frac{R}{t} \times T$, where T is the generation time for each species.

To maximize reliability of PSMC analyses, we removed 20 species with lower-quality heterozygosity information (<18× genome-wide coverage or >25% missing data), following Nadachowska-Brzyska et al (55). For the remaining 325 species, we used the PSMC settings "-N30 -t5 -r5 -p 4+251*1+4+6+10" with a reduced dataset and then scaled results to real time using estimated mutation rate (above) and generation time (56). These parameters ensure a high number of PSMC-based estimates of N_e without changing the overall shape of the PSMC curve (21, 51). Data representing N_e estimates ($\times 10^4$) scaled to real time via PSMC for all 325 species are available in the Dryad Digital Repository (doi:10.5061/dryad.fn2z34tz8).

The PSMC method assumes species come from a single panmictic population. While gene-flow and population structure can potential influence individual N_e estimates over time (18, 57), we adopted a conservative approach of limiting our analysis to the 285 species and periods of the Pleistocene (30 kya–1 mya) where we had full demographic coverage and the highest confidence in PSMC-based estimates of N_e. Our analyses further incorporate species across a broad geographic sampling region and with varying life-history strategies (below), meaning that any geographic variation or life-history strategy (e.g., long-distance migration) which may affect population structure will add additional noise but should not bias our results or interpretations. Germain et al. (21) further assessed the robustness of these estimated N_e trajectories to the sensitivity of PSMC to variation in mutation rates (18), by varying species-specific mutation rates within reasonable ranges. To do so, they sampled 100 estimates of divergence time from the posterior distribution of nodes corresponding to each species, as estimated from MCMCTree, and calculated 100 mutation rates for each species (using fixed substitution rates and generation times). Scaling PSMC outputs using these generated mutation rates produced 100 N_e trajectories per species, which revealed quantitatively similar patterns across the entire dataset (21).

From these criteria, we generated a mean of 173 (±18.2 SD, range = 92–216) point estimates of N_e per species across the full study period. We separated species-specific N_e values into three roughly equal time periods over the Pleistocene (Time 1 = 332 – 30 kya, Time 2 = 665 – 333 kya, Time 3 = 1 Mya – 666 kya) and calculated species-specific means for each period (58). Separating and averaging N_e estimates over these periods provided the most conservative approach to quantifying conservation-relevant, pre-anthropogenic baselines over the past million years. In particular, while PSMC-based estimates of N_e are considered to be most reliable between ~20 kya and 2 Mya, this method provides more detailed representations of short-term demographic fluctuations in the more recent past (i.e., up to ~200kya), whereas point estimates are calculated over longer time frames in the more distant past (18, 59). Thus, averaging a large number of point estimates across relatively large time periods can help chart long-term demographic changes over time while accounting for potential differences in the accuracy of single N_e estimates between the more recent and more distant past (18, 59). We further calculated species-specific mean N_e values for two periods representing the beginning and end of the most recent episode of abrupt climate warming (~147–123 kya) over the past million years (19). These corresponded to 160–140 kya ("warming beginning") and 125–105 kya ("warming end") and represented means of 6.7 (±0.9 SD, range 3–9) and 8.1 (±1.3SD, range = 4–11) point estimates per species.

Our final dataset consisted of full demographic histories for species representing 39 avian orders and geographic distributions ranging from the Arctic to the tropics (21). Demographic histories among n = 34 species currently listed as "threatened" or "near-threatened" exhibit contrasting patterns of N_e increase/decrease over the past million years (21) and are thus unlikely to affect patterns of functional diversity change over time.

Functional Trait Datasets. Morphological, life-history, and ecological trait data for each species were assembled via museum specimens, live-caught individuals,

and published databases following several previous comparative studies in birds (16, 23, 60–62). We used six key morphological and life-history traits identified by Germain et al. (21) as being associated with long-term changes in N_e over the Pleistocene. These six continuous traits were (1) "body mass," mean unsexed body mass (g) or mean of male and female masses, (2) "bill length," mean unsexed bill length (mm) or mean of male and female bill length (exposed culmen), (3) "egg mass," mean mass (g) of fresh eggs, (4) "clutch size," mean number of eggs per clutch, (5) "incubation duration," duration of clutch incubation (days), and (6) "hand-wing index," measured as the distance [mm] between the tip of the first secondary feather to the tip of the longest primary feather, divided by total wing chord length and multiplied by 100. Bill dimensions reflect the trophic or dietary niche (60), and hand-wing index provides a metric of flight efficiency and dispersal ability (63, 64). In total, 263 of the original 285 species had complete information for all six traits and were included in analysis of abundance-weighted representation within functional trait space (below).

We further assigned each species to one of the 11 main zoogeographic realms characterized by Holt et al. (22), via multi-taxon species assemblages. We assigned migratory species to the realm corresponding to their breeding range, and species with ranges extending across multiple realms were assigned to the realm from which the individual sample used for whole-genome sequencing originated.

Categorical traits representing ecological and life-history strategies included broad taxonomic classification (landbirds, raptors, shorebirds, waterbirds, waterfowl), main diet (i.e., aquatic invertebrates, fruit, seeds, invertebrates, nectar, plant material [other than fruit, seeds, or nectar], scavenged material, vertebrates) that comprises >50% of the species' diet, or classified as "omnivore" if none of the food types represent >50% of diet, habitat type (open, semi-open, dense), territoriality (none, weak, strong), migratory strategy (sedentary, partially migratory, migratory), and developmental mode (altricial, semi-precocial or semi-altricial, precocial). Sample sizes for each group within these categorical traits are provided in *SI Appendix*, Table S2; 280 species had complete information for each categorical trait investigated and were thus included in downstream analyses of representation among groups over time (below).

Statistical Analyses.

Abundance-Weighted Occupation of Functional Trait Space. All analyses were performed in *R* 3.6.3 (65). Analysis of changes of occupancy within functional trait space over the three time periods follows the trait probability density (TPD) approach of Carmona et al. (7, 66). We first log-transformed our six key continuous traits and used PCA from correlation matrices to compile them into a functional trait space with a minimum number of dimensions. Each species was represented in this functional trait space by their PCA scores based on their traits. Using the *TPD* package (66), we created community-based (i.e., combining all 263 species) TPDs for Time 1, Time 2, and Time 3. Following Carmona et al. (27), we applied a kernel density function for each species using a multivariate normal distribution centered on the coordinates of the species in functional trait space; bandwidth was selected via the unconstrained bandwidth selectors described in Duong (67). We used the species-specific N_e estimates in each of the three time periods to weight the contribution of each species' kernel to the aggregated TPD function. These TPD functions represent the abundance-weighted occupation of the functional trait space by the avian community in each time period, where all other parameters (i.e., the number of species and trait attributes of each species) remain constant over time. Because we assume that the ecological and morphological traits of each distinct species have remained consistent over the past million years (a relatively brief period in avian evolution (68)), and because our analysis includes the same species composition in each time period, any change in avian functional diversity detected through this TPD approach can be solely attributed to species-specific changes in N_e (8, 46, 66, 69).

We then quantified the overlap-based dissimilarity between the TPD functions of each pair of time periods and compared each dissimilarity to null distributions to test whether changes in the occupation of the functional trait space differed from random expectations. Null distributions were calculated by assigning three random abundance values (representing the three time periods) to each species within their maximum and minimum observed N_e values, creating abundance-weighted TPD functions for each time period and calculating overlap-based dissimilarity between each (as above), and repeating this process for 1000 iterations. Dissimilarity indices between time periods were considered significant if they fell outside of the 95% confidence intervals generated from these distributions.

Finally, we explored temporal changes in the patterns of occupation of the functional space between Time 1 and Time 3. Following Carmona et al. (7), we expressed the TPD functions of each of these time periods in terms of quantiles and subtracted the quantile values of Time 3 from those of Time 1 across all points of the functional space. Negative values of this index represent a lower density of occupation of the particular part of the functional space in the more recent history than in the more distant past (i.e., species with such trait combinations were less abundant in Time 1 than they were in Time 3) and vice versa.

We repeated this process for each of the major zoogeographic realms, where we calculated realm-specific TPD functions and estimated overall dissimilarity (quantile changes) in abundance-weighted functional trait diversity between Time 1 and Time 3. To avoid spurious results for underrepresented realms in our dataset, realms that contained <10 sampled species (Madagascan and Saharo-Arabian) were excluded from comparison of geographic patters of variation in functional diversity over time. We further estimated overall dissimilarity (quantile changes) in abundance-weighted functional trait diversity between the "warming beginning" and "warming end" periods to identify which trait sets exhibited the largest increases and decreases in occupation of functional trait set during this period of abrupt, pre-anthropogenic climate warming.

Representation of Categorical Traits Over Time. We used linear models and multi-model inference to identify the representation (in terms of species-specific abundances) among categorical trait groups over the past million years. For each of the three focal time periods (N_e values scaled within each period), we constructed a global model with each of our ecological traits (taxonomic classification, main diet, habitat type, territoriality, migratory strategy, developmental mode) as predictors. Goodness-of-fit (R^2) of each global model was assessed by the conditional coefficient of determination (70). We ran all possible combinations of these predictors (n = 32 models for each time period) and selected a subset of models which included the best-fitting model (determined via Akaike Information Criterion, AIC) and those with $\Delta AIC \leq 7$ from the best-fitting model (*SI Appendix*, Table S1). We chose this AIC cutoff to ensure that estimates of the links between functional group categories and N_e during each time period were as conservative and inclusive as possible (71). We then averaged parameter estimates for each predictor included in these subsets to create one representative estimate of the relative representation of each trait group in each time period.

Data, Materials, and Software Availability. Demographic data (.txt files representing Ne estimates for 325 species) have been deposited in Dryad (doi:10.5061/dryad.fn2z34tz8). Previously published data on species-specific traits were used for this work (23).

ACKNOWLEDGMENTS. This work is the result of the combined efforts of numerous field biologists and museum staff who contributed samples to the B10k project and AVONET trait database. Funding: This work was supported by grants from the National Natural Science Foundation of China (grant no. 31901214), Independent Research Fund Denmark (grant 8021-00282B: DEMOCHANGE), the Strategic Priority Research Program of the Chinese Academy of Sciences, the International Partnership Program of Chinese Academy of Sciences, the Carlsberg Foundation, the Estonian Research Council (PSG293), and the Villum Foundation (grant no. 25925).

Author affiliations: [a]Center for Macroecology, Evolution, and Climate, Globe Institute, University of Copenhagen, Copenhagen 2100, Denmark; [b]Villum Centre for Biodiversity Genomics, Section for Ecology and Evolution, Department of Biology, University of Copenhagen, Copenhagen 2100, Denmark; [c]BGI-Shenzhen, Shenzhen 518083, China; [d]Center for Evolutionary & Organismal Biology, Zhejiang University School of Medicine, Hangzhou 310058, China; [e]Liangzhu Laboratory, Zhejiang University Medical Center, Hangzhou 311121, China; [f]Département de Biologie, École Normale Supérieure de Lyon, Université Claude Bernard Lyon 1, Université de Lyon, Lyon 69342 Cedex 07, France; [g]Institute of Ecology and Earth Sciences, University of Tartu, Tartu 51005, Estonia; [h]College of Life Sciences, University of Chinese Academy of Sciences, Beijing 100101, China; [i]Department of Vertebrate Zoology, National Museum of Natural History Smithsonian Institution, Washington 20560, DC; [j]Department of Life Sciences, Imperial College London, Ascot SL5 7PY, UK; [k]Center for Global Mountain Biodiversity, Globe Institute, University of Copenhagen, Copenhagen 2100, Denmark; [l]Institute of Ecology, Peking University, Beijing 100871, China; [m]Danish Institute for Advanced Study, University of Southern Denmark, Odense 5230, Denmark; [n]Institute of Zoology, Key Laboratory of Zoological Systematics and Evolution, Chinese Academy of Sciences, Beijing 100101, China; [o]Natural History Museum of Denmark, University of Copenhagen, Copenhagen 2100, Denmark; [p]Center for Evolutionary Hologenomics, Globe Institute University of

Copenhagen, Copenhagen 1353, Denmark; [q]Department of Natural History, University Museum, Norwegian University of Science and Technology, Trondheim 7491, Norway; and [r]State Key Laboratory of Genetic Resources and Evolution, Kunming Institute of Zoology, Chinese Academy of Sciences, Kunming 650223, China

1. IPBES, Global assessment report on biodiversity and ecosystem services of the Intergovernmental science-policy platform on biodiversity and ecosystem services, E.S. Brondizio, J. Settele, S. Diaz, H.T. Ngo, Eds. (IPBES secretariat, 2019), 21 June 2021.
2. D. A. Fordham *et al.*, Using paleo-archives to safeguard biodiversity under climate change. *Science* **369**, eabc5654 (2020).
3. T. H. Oliver, M. D. Morecroft, Interactions between climate change and land use change on biodiversity: Attribution problems, risks, and opportunities. *WIREs Clim. Change* **5**, 317–335 (2014).
4. S. M. Smart *et al.*, Clarity or confusion? – Problems in attributing large-scale ecological changes to anthropogenic drivers. *Ecol. Indic.* **20**, 51–56 (2012).
5. D. E. Bowler *et al.*, Mapping human pressures on biodiversity across the planet uncovers anthropogenic threat complexes. *People Nat.* **2**, 380–394 (2020).
6. R. S. C. Cooke, F. Eigenbrod, A. E. Bates, Projected losses of global mammal and bird ecological strategies. *Nat. Commun.* **10**, 2279 (2019).
7. C. P. Carmona *et al.*, Erosion of global functional diversity across the tree of life. *Sci. Adv.* **7**, eabf2675 (2021).
8. C. P. Carmona, F. de Bello, N. W. H. Mason, J. Lepš, Traits without borders: Integrating functional diversity across scales. *Trends Ecol. Evol.* **31**, 382–394 (2016).
9. S. Bauer, B. J. Hoye, Migratory animals couple biodiversity and ecosystem functioning worldwide. *Science* **344**, 1242552 (2014).
10. D. U. Hooper *et al.*, A global synthesis reveals biodiversity loss as a major driver of ecosystem change. *Nature* **486**, 105–108 (2012).
11. S. Naeem, Species redundancy and ecosystem reliability. *Cons. Biol.* **12**, 39–45 (1998).
12. H. Hillebrand *et al.*, Biodiversity change is uncoupled from species richness trends: Consequences for conservation and monitoring. *J. Appl. Ecol.* **55**, 169–184 (2018).
13. B. Leung *et al.*, Clustered versus catastrophic global vertebrate declines. *Nature* **588**, 267–271 (2020).
14. L. M. Hallett, E. C. Farrer, K. N. Suding, H. A. Mooney, R. J. Hobbs, Tradeoffs in demographic mechanisms underlie differences in species abundance and stability. *Nat. Commun.* **9**, 5047 (2018).
15. K. V. Rosenberg *et al.*, Decline of the north american avifauna. *Science* **366**, 120–124 (2019).
16. D. Sol *et al.*, The worldwide impact of urbanisation on avian functional diversity. *Ecol. Lett.* **23**, 962–972 (2020).
17. D. Nogués-Bravo *et al.*, Cracking the code of biodiversity responses to past climate change. *Trends Ecol. Evol.* **33**, 765–776 (2018).
18. H. Li, R. Durbin, Inference of human population history from individual whole-genome sequences. *Nature* **475**, 493–496 (2011).
19. C. W. Snyder, Evolution of global temperature over the past two million years. *Nature* **538**, 226–228 (2016).
20. F. Botta, D. Dahl-Jensen, C. Rahbek, A. Svensson, D. Nogués-Bravo, Abrupt change in climate and biotic systems. *Curr. Biol.* **29**, R1045–R1054 (2019).
21. R. R. Germain *et al.*, Species-specific traits mediate avian demographic responses under past climate change. bioRxiv [Preprint]. https://www.biorxiv.org/content/10.1101/2022.08.16.504093v1 (Accessed 16 August 2022), 2022.08.16.504093.
22. B. G. Holt *et al.*, An Update of Wallace's Zoogeographic Regions of the World. *Science* **339**, 74–78 (2013).
23. J. A. Tobias *et al.*, AVONET: Morphological, ecological and geographical data for all birds. *Ecol. Lett.* **25**, 581–597 (2022).
24. C. H. Sekercioglu, Increasing awareness of avian ecological function. *Trends Ecol. Evol.* **21**, 464–471 (2006).
25. S. C. Stearns, The evolution of life history traits: A critique of the theory and a review of the data. *Annu. Rev. Ecol. Evol. Syst.* **8**, 145–171 (1977).
26. K. Thorup *et al.*, Response of an Afro-Palearctic bird migrant to glaciation cycles. *Proc. Natl. Acad. Sci. U.S.A.* **118**, e2023836118 (2021).
27. C. P. Carmona *et al.*, Fine-root traits in the global spectrum of plant form and function. *Nature* **597**, 683–687 (2021).
28. S. Díaz *et al.*, The global spectrum of plant form and function. *Nature* **529**, 167–171 (2016).
29. D. Tilman, D. Wedin, J. Knops, Productivity and sustainability influenced by biodiversity in grassland ecosystems. *Nature* **379**, 718–720 (1996).
30. D. Tilman *et al.*, The influence of functional diversity and composition on ecosystem processes. *Science* **277**, 1300–1302 (1997).
31. D. Tilman, C. L. Lehman, K. T. Thomson, Plant diversity and ecosystem productivity: Theoretical considerations. *Proc. Natl. Acad. Sci. U.S.A.* **94**, 1857–1861 (1997).
32. S. Naeem, S. Li, Biodiversity enhances ecosystem reliability. *Nature* **390**, 507–509 (1997).
33. A. Hector *et al.*, Plant diversity and productivity experiments in european grasslands. *Science* **286**, 1123–1127 (1999).
34. J. S. Rosenfeld, Functional redundancy in ecology and conservation. *Oikos* **98**, 156–162 (2002).
35. C. R. Biggs *et al.*, Does functional redundancy affect ecological stability and resilience? A review and meta-analysis. *Ecosphere* **11**, e03184 (2020).
36. A. Toussaint *et al.*, Extinction of threatened vertebrates will lead to idiosyncratic changes in functional diversity across the world. *Nat. Commun.* **12**, 5162 (2021).
37. H. M. Pereira *et al.*, Essential Biodiversity Variables. *Science* **339**, 277–278 (2013).
38. L. M. Bland, D. A. Keith, R. M. Miller, N. J. Murray, J. P. Rodriguez, *Guidelines for the Application of IUCN Red List of Ecosystems Categories and Criteria* (Version 1.0, IUCN, Gland, Switzerland, 2017).
39. T. M. Blackburn, K. J. Gaston, Animal body size distributions: Patterns, mechanisms and implications. *Trends Ecol. Evol.* **9**, 471–474 (1994).
40. J. L. Gill, Ecological impacts of the late Quaternary megaherbivore extinctions. *New Phytol.* **201**, 1163–1169 (2014).
41. Y. Malhi *et al.*, Megafauna and ecosystem function from the Pleistocene to the Anthropocene. *Proc. Natl. Acad. Sci. U.S.A.* **113**, 838–846 (2016).
42. S. C. Stearns, *The Evolution of Life Histories* (Oxford University Press, 1992).
43. A. Fromm, S. Meiri, Big, flightless, insular and dead: Characterising the extinct birds of the Quaternary. *J. Biogeogr.* **48**, 2350–2359 (2021).
44. J. B. C. Jackson, K. G. Johnson, Measuring past biodiversity. *Science* **293**, 2401–2404 (2001).
45. J. D. Sigwart *et al.*, Measuring biodiversity and extinction–Present and past. *Integ. Comp. Biol.* **58**, 1111–1117 (2018).
46. S. Feng *et al.*, Dense sampling of bird diversity increases power of comparative genomics. *Nature* **587**, 252–257 (2020).
47. E. Santiago *et al.*, Recent demographic history inferred by high-resolution analysis of linkage disequilibrium. *Mol. Biol. Evol.* **37**, 3642–3653 (2020).
48. J. A. Tobias, A bird in the hand: Global-scale morphological trait datasets open new frontiers of ecology, evolution and ecosystem science. *Ecol. Lett.* **25**, 573–580 (2022).
49. M. W. Cadotte, K. Carscadden, N. Mirotchnick, Beyond species: Functional diversity and the maintenance of ecological processes and services. *J. Appl. Ecol.* **48**, 1079–1087 (2011).
50. A. McKenna *et al.*, The genome analysis toolkit: A MapReduce framework for analyzing next-generation DNA sequencing data. *Genome Res.* **20**, 1297–1303 (2010).
51. K. Nadachowska-Brzyska, C. Li, L. Smeds, G. Zhang, H. Ellegren, Temporal dynamics of Avian populations during pleistocene revealed by whole-genome sequences. *Curr. Biol.* **25**, 1375–1380 (2015).
52. Z. Yang, PAML: A program package for phylogenetic analysis by maximum likelihood. *Comput. Appl. Biosci.* **13**, 555–556 (1997).
53. F. Forest, Calibrating the tree of life: Fossils, molecules and evolutionary timescales. *Ann. Bot.* **104**, 789–794 (2009).
54. S. A. Magallón, Dating lineages: Molecular and paleontological approaches to the temporal framework of clades. *Int. J. Plant Sci.* **165**, S7–S21 (2004).
55. K. Nadachowska-Brzyska, R. Burri, L. Smeds, H. Ellegren, PSMC analysis of effective population sizes in molecular ecology and its application to black-and-white Ficedula flycatchers. *Mol. Ecol.* **25**, 1058–1072 (2016).
56. J. P. Bird *et al.*, Generation lengths of the world's birds and their implications for extinction risk. *Cons. Biol.* **34**, 1252–1261 (2020).
57. O. Mazet, W. Rodríguez, S. Grusea, S. Boitard, L. Chikhi, On the importance of being structured: instantaneous coalescence rates and human evolution–Lessons for ancestral population size inference?. *Heredity* **116**, 362–371 (2016).
58. A. Brüniche-Olsen, K. F. Kellner, J. L. Belant, J. A. DeWoody, Life-history traits and habitat availability shape genomic diversity in birds: implications for conservation. *Proc. R. Soc. B* **288**, 20211441 (2021).
59. K. Nadachowska-Brzyska, M. Konczal, W. Babik, Navigating the temporal continuum of effective population size. *Methods Ecol. Evol.* **13**, 22–41 (2022).
60. A. L. Pigot *et al.*, Macroevolutionary convergence connects morphological form to ecological function in birds. *Nat. Ecol. Evol.* **4**, 230–239 (2020).
61. C. Sheard *et al.*, Ecological drivers of global gradients in avian dispersal inferred from wing morphology. *Nat. Commun.* **11**, 2463 (2020).
62. J. A. Tobias, A. L. Pigot, Integrating behaviour and ecology into global biodiversity conservation strategies. *Philos. Trans. R. Soc. Lond. B* **374**, 20190012 (2019).
63. B. C. Weeks, Morphological adaptations linked to flight efficiency and aerial lifestyle determine natal dispersal distance in birds. *Funct. Ecol.*, in press.
64. S. Claramunt, Flight efficiency explains differences in natal dispersal distances in birds. *Ecology* **102**, e03442 (2021).
65. R Development Core Team, *R: A Language and Environment for Statistical Computing* (Version 3.6.3, R Foundation for Statistical Computing, Vienna, Austria, 2020).
66. C. P. Carmona, F. de Bello, N. W. H. Mason, J. Lepš, Trait probability density (TPD): Measuring functional diversity across scales based on TPD with R. *Ecology* **100**, e02876 (2019).
67. T. Duong, ks: Kernel density estimation and kernel discriminant analysis for multivariate data in R. *J. Stat. Softw.* **21**, 1–16 (2007).
68. W. Jetz, G. H. Thomas, J. B. Joy, K. Hartmann, A. O. Mooers, The global diversity of birds in space and time. *Nature* **491**, 444–448 (2012).
69. L. M. Callender-Crowe, R. S. Sansom, Osteological characters of birds and reptiles are more congruent with molecular phylogenies than soft characters are. *Zool. J. Linn. Soc.* **194**, 1–13 (2022).
70. S. Nakagawa, H. Schielzeth, A general and simple method for obtaining R2 from generalized linear mixed-effects models. *Methods Ecol. Evol.* **4**, 133–142 (2013).
71. K. Burnham, D. Anderson, *Model Selection and Multi-Model Inference: A practical information-theoretic approach* (Springer, 2002).